THE ASTROPHYSICAL JOURNAL, 204:L131–L134, 1976 March 15

H_2CO EMISSION AT 2 MILLIMETERS IN DARK CLOUDS

N. J. EVANS II
Owens Valley Radio Observatory, California Institute of Technology; and
Department of Astronomy, The University of Texas at Austin

AND

M. L. KUTNER
Goddard Institute for Space Studies, New York; and Department of Physics, Rensselaer Polytechnic Institute
Received 1975 October 15; revised 1975 December 4

ABSTRACT

The $2_{12} \rightarrow 1_{11}$ transition of H_2CO at 2 mm wavelength has been detected at three positions in dark clouds. This confirms predictions based on 2 cm H_2CO absorption studies. The 2 mm radiation temperatures, together with the 2 cm data and recently computed cross sections for H_2–H_2CO collisions, are used to deduce cloud conditions. These in turn are used to predict the strengths of emission lines from CS and HCN.
Subject heading: interstellar: molecules

I. INTRODUCTION

Surveys of the 6 cm absorption line of H_2CO have demonstrated that H_2CO is present in many dark clouds (Palmer *et al.* 1969; Dieter 1973; Minn and Greenberg 1973). Nonetheless, earlier searches in such clouds for the 2 mm H_2CO line had proven fruitless (Kutner 1972). Because millimeter emission lines from other molecules, notably HCN and CS, have also not been seen in dark clouds, it has been concluded that dark clouds lack the excitation conditions, especially the hydrogen density, which produce these lines in molecular clouds associated with H II regions. However, one could equally well explain the absence of emission from CS and HCN as due to a chemical, rather than a physical, difference between dark clouds and molecular clouds near H II regions. This ambiguity is not present for H_2CO, because its existence and approximate column density can be established by studies of the absorption lines at 6 cm and 2 cm. In fact, comparative studies of these two absorption lines have indicated that high densities and substantial trapping do exist in at least some parts of dark clouds (Evans *et al.* 1975, hereafter denoted EZMS). The ratio of absorption strengths in the 2 cm and 6 cm lines was suggested as a probe of density in dark clouds. As an unavoidable consequence of the strong 2 cm absorption, EZMS predicted that 2 mm emission lines with radiation temperatures ~0.5 K should be detectable from positions in the Taurus cloud and L134 N. The former cloud, studied by Kutner (1973), lies in a cluster of dark clouds near L1529 (Lynds 1962). The cloud referred to as L134 N by EZMS and others appears to be L183.

II. OBSERVATIONS

The observations were made with the 16 foot (5 m) radio telescope of the M.W.O.,[1] Ft. Davis, Texas. The half-power beamwidth (HPBW) at 2 mm was 2′. The 40 channel filter bank gave a velocity resolution of 0.53 km s^{-1}. Calibration was accomplished by a rotating chopper wheel with the scale of radiation temperatures set by the method of Davis and Vanden Bout (1973). Sky conditions were clear and stable; the absolute calibration should be good to 10 percent ($\pm$ 1 σ).

The profiles of $2_{12} \rightarrow 1_{11}$ H_2CO emission are shown in Figure 1. Two positions in the Taurus dark cloud, separated by 2′ in right ascension, and one position in L134 N were observed. To select a region of relatively uniform 2 cm absorption, the positions for observation

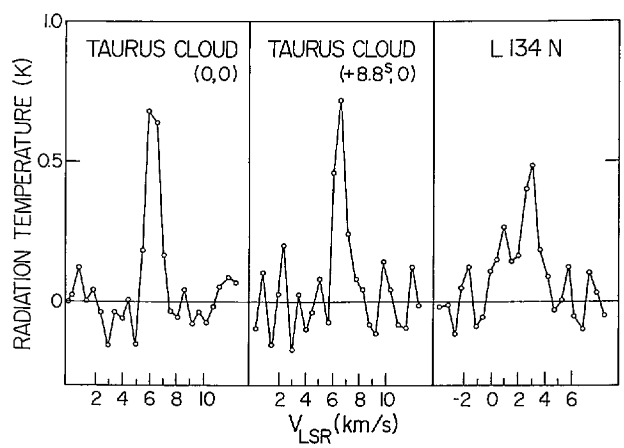

FIG. 1.—Spectra of the $2_{12} \rightarrow 1_{11}$ transition from two positions in the Taurus cloud and one position in L134 N. The (0,0) position in Taurus is $\alpha = 04^h29^m43^s.4$; $\delta = +24°16'55''$. The position in L134 N is $\alpha = 15^h51^m30^s.0$; $\delta = -2°43'31''$ (1950 coordinates).

[1] The Millimeter Wave Observatory is operated by the Electrical Engineering Research Laboratory of the University of Texas at Austin, with support from the National Aeronautics and Space Administration, the National Science Foundation, and McDonald Observatory.

at 2 mm were chosen midway between two adjacent 2 cm positions with equally strong absorption lines and no velocity gradients. Because the 2 cm data were also taken with a 2′ beam, a region which is uniform on this scale should have been sampled by this technique. The velocity and width of the 2 mm lines in the Taurus cloud agree very well with those of the 2 cm lines. In L134 N, the velocity at 2 mm differs from the 2 cm velocity by 0.5 km s^{-1}, and the shape may be different. There was some marginal evidence for a line-width variation in the 2 cm data; hence this may not be as uniform a region as the one in Taurus.

In discussing radiation temperature, we use the notation of EZMS, where ΔT_{Rij} represents the peak radiation temperature in a line which connects levels i and j, and the four lowest levels of ortho-formaldehyde are labeled sequentially in order of increasing energy. From Figure 1, the peak radiation temperature at 2 mm, $\Delta T_{R13} = 0.7 \pm 0.1$ K at the two positions in the Taurus cloud. The 2 cm radiation temperature will be taken as $\Delta T_{R34} = -0.28 \pm 0.04$ K, an average of the 2 cm positions; the error is a representative random error ($\pm 1\ \sigma$) at a given position and covers the range of values at different positions. While ΔT_{R34} is also -0.27 ± 0.04 K in L134 N, ΔT_{R13} is 0.5 K, somewhat less than in Taurus.

III. DISCUSSION

a) *Cross Sections*

The detection of 2 mm emission lines confirms the predictions of EZMS. They found that enhancement of cross sections from *both* levels of the $J = 1$ doublet into the lower level of the $J = 2$ doublet (models II and III of EZMS) was required to explain the observations. Recently the cross sections for He–H_2CO collisions have been determined in an accurate quantum-mechanical calculation (Garrison *et al.* 1975); these should also provide a good representation of the H_2–H_2CO cross sections. While the theoretical cross sections differ substantially from those used by EZMS (in particular, transitions to the $J = 3$ doublet play a crucial role in cooling the $J = 1$ and $J = 2$ doublets), the predicted excitation temperatures, T_{13} and T_{34}, are very similar to those predicted by empirical model II or III of EZMS. Furthermore, trapping calculations have shown that the theoretical cross sections also predict ΔT_{R13} and ΔT_{R34} which are very similar to those predicted by model III, but predict somewhat different 6 cm radiation temperatures, ΔT_{R12}. Thus the theoretical cross sections generally introduce few changes into the interpretation of EZMS, but they do allow the removal of one major source of ambiguity in the interpretation of H_2CO observations. We have used the rates given by Garrison *et al.* (1975) for kinetic temperature, $T_K =$ 15 K in the analysis described below; CO observations suggest $T_K \sim 12$ K at the positions in question.

b) *Cloud Models*

Besides cross section uncertainties, the other primary sources of ambiguity in interpreting observations have been the treatment of radiative transport and the related questions of cloud models. This is especially severe for linear molecules where, typically, all transitions are optically thick and the effects of collisions and trapping cannot be easily separated (cf. Goldreich and Kwan 1974). H_2CO offers substantial advantages in this regard, as both optically thick (2 mm) and optically thin (2 cm) transitions arise from the same state—in this case, level 3. This makes it possible to derive separately the hydrogen density, n_{H_2}, and the ortho-H_2CO column density, $nL(H_2CO)$.

We have used cloud models with constant density and temperature and have treated the radiative transport in the large velocity gradient (LVG) approximation, with both spherical [$v(r) \sim r$] and slab geometries and a velocity gradient of 1 km s^{-1} pc^{-1}. Figure 2 shows the predicted radiation temperatures. To obtain a solution for n_{H_2} and $nL(H_2CO)$, one uses the observed ΔT_{R13} to obtain values of n_{H_2}, ΔT_{R34}, and ΔT_{R12} for each $nL(H_2CO)$. This was done for a grid of $nL(H_2CO)$ spaced by factors of $2^{1/4}$ and extending from 4.4×10^{13} cm^{-2} to 12.5×10^{13} cm^{-2} (not all of these are shown in Fig. 2). The results for $\Delta T_{R13} = 0.7$ K are shown in Figure 3. The effect of trapping in lowering the hydrogen density required to produce a given 2 mm line is apparent; the dependence of the 2 cm and 6 cm absorption strength on the trapping, or $nL(H_2CO)$, is also apparent. Therefore, the observed ΔT_{R34} determines $nL(H_2CO)$ and thus n_{H_2}. The solutions from Figure 3, and from similar figures constructed for $\Delta T_{R13} = 0.5$ and 0.9 K, are given in Table 1.

Also listed in Table 1 are the predicted ΔT_{R12}; because the ΔT_{R12} listed in Table 5 of EZMS were measured with a large beam (6′–10′), and because the positions of deepest 2 cm absorption, hence highest n_{H_2}, were chosen for the search at 2 mm, the fact that the models predict

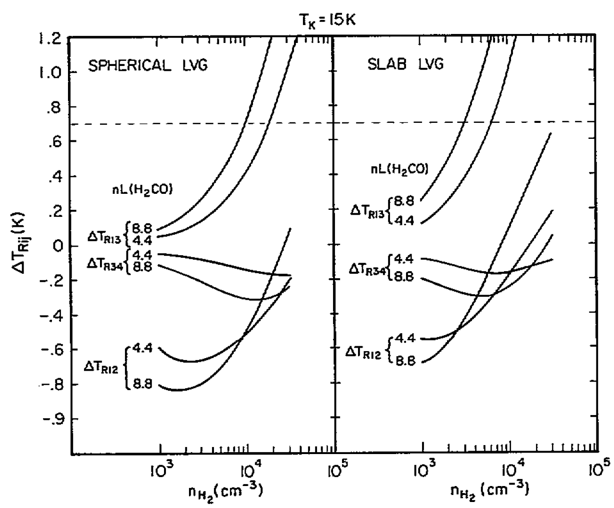

FIG. 2.—Predicted radiation temperatures as a function of hydrogen density for two values of $nL(H_2CO)$: 4.4×10^{13} cm^{-2} and 8.8×10^{13} cm^{-2}. Theoretical collision rates for $T_K = 15$ K were used in cloud models with large velocity gradients (LVG) and both spherical and slab geometries. The dashed line indicates the observed 2 mm radiation temperature, ΔT_{R13}, in the Taurus cloud.

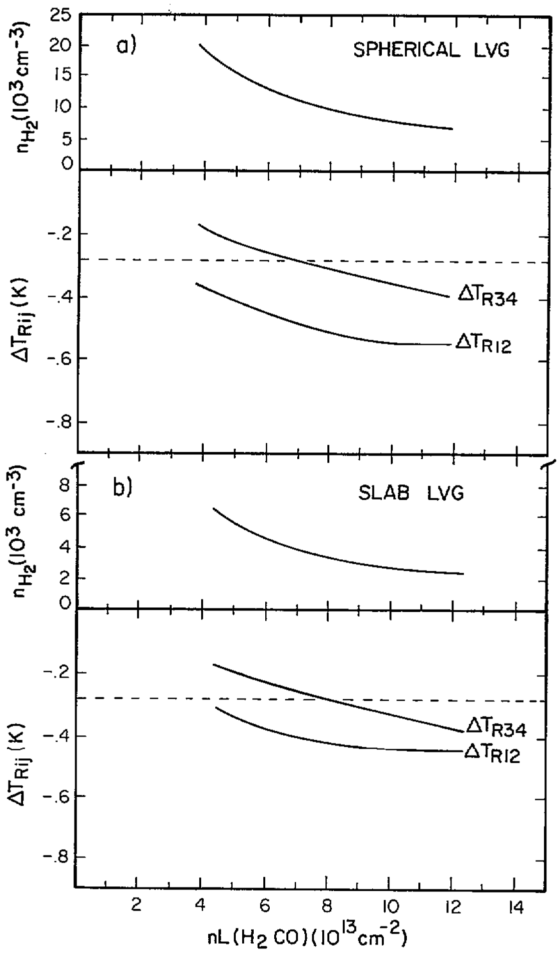

FIG. 3.—The bottom graph of Fig. 3*a* shows ΔT_{R34} and ΔT_{R12}, 2 cm and 6 cm radiation temperature, versus $nL(H_2CO)$ subject to the constraint that $\Delta T_{R13} = 0.7$ K. The dashed line shows the value of ΔT_{R34} observed in the Taurus cloud. From the column density where theory and observations agree, the hydrogen density (*top graph*) is also determined. Fig. 3*b* presents the same quantities predicted by a slab LVG calculation.

somewhat less absorption at 6 cm than is seen is not surprising. Table 1 clearly shows the weakening of the 6 cm absorption as n_{H_2} increases. Maps of the 6 cm line with a smaller beam would be helpful in checking this picture.

The solution for $nL(H_2CO)$ of $\sim 8 \times 10^{13}$ cm^{-2} does not change the fractional abundance of H_2CO of 4×10^{-9} nor the $H_2{}^{12}CO/H_2{}^{13}CO$ ratio derived by EZMS. A column density $nL(H_2{}^{13}CO) = 8.8 \times 10^{11}$ cm^{-2} predicts a 6 cm antenna temperature of -0.011 K, when corrected for hyperfine dilution; and EZMS observed -0.0098 K. The main uncertainty here is due to the 10′ beam used for the $H_2{}^{13}CO$ observations.

c) Errors and Uncertainties

The errors in Table 1 reflect only the errors in ΔT_{R34} ($\pm 1\ \sigma$). The effect of errors in ΔT_{R13} may be seen by comparing solutions for $\Delta T_{R13} = 0.5$ K and 0.9 K, representing $\pm 2\ \sigma$ errors for the Taurus result of $\Delta T_{R13} = 0.7$ K, or equivalently, ± 30 percent calibration errors. The solutions for $\Delta T_{R13} = 0.5$ K would nominally apply to the L134 N cloud, but caution is required because the velocity and line-width agreement was poor in this case. For the Taurus cloud, the column density, $nL(H_2CO)$, is very insensitive to errors in ΔT_{R13} or to differences in cloud models. The hydrogen density, however, does depend quite strongly on the value of ΔT_{R13} and on the choice of a sphere or a slab. Within $\pm 1\ \sigma$ errors on the observations, it is the geometrical model that provides the limiting uncertainties.

As mentioned above, both slab and spherical geometries employ the large velocity gradient (LVG) approximation. Although no calculations with a microturbulent cloud model have been done with the theoretical cross sections of Garrison *et al.* (1975), such calculations were presented by EZMS for their empirical cross section models. New calculations indicate that the spherical LVG calculation with empirical cross sections provides an excellent approximation to a microturbulent calculation at $nL(H_2CO) = 4.4 \times 10^{13}$ cm^{-2}. Thus a spherical LVG calculation with the theoretical cross sections should give a fair idea of what a microturbulent calculation would predict, especially since the theoretical cross sections and the empirical model III cross sections also produced very similar results in an LVG calculation. If differences between microturbulent and spherical LVG models are more significant at $nL(H_2CO) = 8 \times 10^{13}$ cm^{-2}, then a microturbulent model would have somewhat higher densities than the spherical LVG model.

d) Molecular Abundances in Dark Clouds

Returning to the question of molecular abundances in dark clouds, we recall that the failure to detect HCN and CS in dark clouds has often been attributed to

TABLE 1

SOLUTIONS FROM FIGURE 3

	SPHERICAL LVG			SLAB LVG		
ΔT_{R13} (K)	n_{H_2} (10^3 cm^{-3})	$nL(H_2CO)$ (10^{13} cm^{-2})	ΔT_{R12} (K)	n_{H_2} (10^3 cm^{-3})	$nL(H_2CO)$ (10^{13} cm^{-2})	ΔT_{R12} (K)
0.5..........	6.5±1.5	8.5±1.5	−0.65±0.04	2.0±0.4	9.7±1.9	−0.58±0.04
0.7 (Taurus)..	11.0±2.5	7.5±1.5	−0.48±0.05	3.5±0.7	8.0±1.6	−0.43±0.03
0.9..........	16.0±3.0	7.4±1.4	−0.35±0.03	4.7±1.4	7.9±1.5	−0.30±0.02

densities insufficient for excitation. The present results allow a critical reexamination of this hypothesis for the positions where 2 mm H_2CO emission is seen. Trapping calculations were performed with the cloud conditions derived above and with theoretical collision rates for CS (Lucas 1974) and HCN (Green and Thaddeus 1975). If $n(\mathrm{CS}) = n(\mathrm{H_2CO})$, then $\Delta T_{R01} \gtrsim 1.8$ K and $\Delta T_{R12} \gtrsim 0.8$ K are predicted for CS. An upper limit of $\Delta T_{R01} < 0.5$ K in L134 N (Turner *et al.* 1973) suggests that $n(\mathrm{CS}) < 0.25\ n(\mathrm{H_2CO})$. For HCN, $\Delta T_{R01} \sim 1.0$ K was predicted if $n(\mathrm{HCN}) = n(\mathrm{H_2CO})$. The abundance of CS is similar to that of H_2CO in clouds near H II regions (Turner *et al.* 1973; Liszt and Linke 1975). The abundance of HCN relative to H_2 in molecular clouds near H II regions is poorly known; estimates range from 8×10^{-10} (Clark, Buhl, and Snyder 1974) to 3×10^{-8}–10^{-5} (Kwan and Scoville 1975). If the latter estimate is correct, sensitive searches for HCN in dark clouds could limit its abundance to 1/30 that in molecular clouds near H II regions. Thus observations of CS and HCN in the Taurus cloud and in L134 N would lead to information on whether the chemistries that prevail in dark clouds are different from those in clouds near H II regions.

While this paper was in press, Martin and Barrett (1975) reported detection of CS from a position 1′ from our position in the Taurus cloud. While their value of $\Delta T_{R12} = 0.53$ K is readily explained with $n(\mathrm{CS})/n(\mathrm{H_2CO}) = 0.5$–$0.7$, their value of ΔT_{R01} is much stronger than expected at these relative abundances and the cloud conditions in Table 1. Because their calibration for the $1 \rightarrow 0$ line seems less secure, the above relative abundances are probably correct.

IV. CONCLUSIONS

The detection of 2 mm emission lines from H_2CO at three dark-cloud positions confirms the predictions of EZMS. The present results indicate densities in the Taurus cloud positions of $n_{H_2} \sim 10^4$ cm^{-3}. The suggestions of EZMS that $n(\mathrm{H_2CO})/n_{H_2} \sim 4 \times 10^{-9}$ and $H_2{}^{12}CO/H_2{}^{13}CO \sim 90$ in Taurus and L134N are supported by the present results. The use of cloud conditions determined from H_2CO in models for CS and HCN emission indicate that if those molecules have abundances equal to H_2CO, they should be easily detectable. An existing upper limit on the $1 \rightarrow 0$ CS line in L134 N suggests that $n(\mathrm{CS}) < 0.25\ n(\mathrm{H_2CO})$, in apparent distinction to the case in molecular clouds near H II regions, where $n(\mathrm{CS}) \sim n(\mathrm{H_2CO})$.

These observations should be distinguished from detections of 2 mm H_2CO emission in active dark cloud regions, as indicated by CO or ^{13}CO hot spots, far-infrared emission, or visible nebulosity—for example, the Ophiuchus cloud (Encrenaz 1974). The present results show that dark clouds with no distinctive optical features or marked CO enhancement may also produce emission from millimeter lines, indicating the existence of dense regions. The small-scale (1′–2′) variations in ΔT_{R34} noted by EZMS suggest a region of fragmentation and local contraction; such regions are the logical precursors of dark cloud regions with infrared objects, heated CO, and compact H II regions.

We wish to thank N. Z. Scoville for the use of computer programs for the LVG trapping case. Research in radio astronomy at the Owens Valley Radio Observatory is supported by the National Science Foundation under grant GP-30400-X1 and by the Office of Naval Research under contract N00014-67-A-0094-0019. N. J. E. also acknowledges support from NSF grant MPS 72-05070. One of us (M. L. K.) was partially supported by NASA grant NGR-33-008-191.

REFERENCES

Clark, F. O., Buhl, D., and Snyder, L. E. 1974, *Ap. J.*, **190**, 545–556.
Davis, J. H., and Vanden Bout, P. 1973, *Ap. Letters*, **15**, 43–47.
Dieter, N. H. 1973, *Ap. J.*, **183**, 449–468.
Encrenaz, P. J. 1974, *Ap. J. (Letters)*, **189**, L135.
Evans, N. J., II, Zuckerman, B., Morris, G., and Sato, T. 1975, *Ap. J.*, **196**, 433–456 (EZMS).
Garrison, B. J., Lester, W. A., Jr., Miller, W. H., and Green, S. 1975, *Ap. J. (Letters)*, **200**, L175.
Goldreich, P., and Kwan, J. 1974, *Ap. J.*, **189**, 441.
Green, S., and Thaddeus, P. 1974, *Ap. J.*, **191**, 653–657.
Kutner, M. L. 1972, unpublished dissertation, Columbia University.
———. 1973, in *Molecules in the Galactic Environment*, ed. M. A. Gordon and L. E. Snyder (New York: Wiley).
Kwan, J., and Scoville, N. 1975, *Ap. J. (Letters)*, **195**, L85–L88.
Liszt, H. S., and Linke, R. A. 1975, *Ap. J.*, **196**, 709–717.
Lucas, R., 1974, *Astr. and Ap.*, **36**, 465.
Lynds, B. T. 1962, *Ap. J. Suppl.*, **7**, 1.
Martin, R. N., and Barrett, A. H. 1975, *Ap. J. (Letters)*, **202**, L83.
Minn, Y. K., and Greenberg, J. H. 1973, *Astr. and Ap.*, **22**, 13.
Palmer, P., Zuckerman, B., Buhl, D., and Snyder, L. E. 1969, *Ap. J. (Letters)*, **156**, L147–L150.
Turner, B. E., Zuckerman, B., Palmer, P., and Morris, M. 1973, *Ap. J.*, **186**, 123.

N. J. EVANS II: Department of Astronomy, University of Texas, Austin, TX 78712

M. L. KUTNER: Department of Physics, Rensselaer Polytechnic Institute, Troy, NY 12181